Original Article

Received: 2023-01-27
Accepted: 2023-04-08

BCCR
2022, No 4, Vol 14 :185-197
www.bccrjournal.com

Computer-aided peptide-based drug design for inositol-requiring enzyme 1

Alireza Ghanbari[1], Amir Norouzy[2], Negar Balmeh[3], Najaf Allahyari Fard[3*], Mohammad Amin Moosavi[1*]

ABSTRACT

Inositol-requiring enzyme 1 (IRE1), an endoplasmic reticulum (ER) transmembrane protein with both kinase and endoribonuclease activities, plays an essential role during ER stress and its subsequent unfolded protein response (UPR). Recent evidence shows IRE1 signaling contributes to tumorigenesis and cancer progression, pointing to the therapeutic importance of this conserved arm of the UPR. Here, we employed different computational tools to design and predict short peptides with the capability of disrupting IRE1 dimerization/oligomerization, as a strategy for inhibiting its Kinase and RNase activities. A mutation-based peptide library was constructed using mCSM-PPI2 and OSPREY 3.0. The molecular interaction analyses between the designed peptides and IRE1 protein were conducted using the HADDOCK 2.2 online server, followed with molecular dynamics analysis by the GROMACS 2020 package. We then selected short peptide candidates that exhibited high affinity and best predicted physicochemical properties in complex with IRE1. Finally, online servers, such as ToxinPred and AllerTop, were used to identify the best peptide candidates that showed no significant allergenic or cytotoxic properties. These rational designed peptides with the capability of binding to IRE1 oligomerization domain can be considered as potential drug candidates for disrupting IRE1 activity in cancer and related diseases, pending for further validation by in silico and experimental studies.

Keywords: Bioinformatics, cancer, drug design, inositol-requiring enzyme 1, short peptides.

1. Department of Molecular Medicine, Institute of Medical Biotechnology (IMB), National Institute of Genetic Engineering and Biotechnology (NIGEB), P.O Box 161/14965, Tehran, Iran.
2. Department of Bioprocess Engineering, National Institute of Genetic Engineering and Biotechnology (NIGEB), P.O. Box: 161/14965, Tehran, Iran.
3.Department of Systems Biotechnology, National Institute of Genetic Engineering and Biotechnology (NIGEB), P.O. Box: 161/14965, Tehran, Iran.

Corresponding authors:
Allahyari Fard N, Ph.D.,
National Institute of Genetic Engineering and Biotechnology (NIGEB),
P.O. Box: 161/14965, Tehran, Iran.
Email: allahyar@nigeb.ac.ir
Moosavi MA, Ph.D.,
National Institute of Genetic Engineering and Biotechnology (NIGEB),
P.O. Box: 161/14965, Tehran, Iran.
Email: a-moosavi@nigeb.ac.ir

INTRODUCTION:

Despite the progression in etiology and treatment of cancer, it remains the second leading cause of death worldwide (1). Obtaining more knowledge about the contribution of risk factors and molecular signaling pathways to cancer formation and treatment are essential to help in improving current preventive and therapeutic strategies for this disease (2, 3).

The endoplasmic reticulum (ER) serves as an important organelle for the synthesis and post-translational modification of more than 30% of all cellular proteins (4). Perturbations in protein folding triggered by stressful factors, such as calcium levels, redox status, and glycosylation, may result in the accumulation of misfolded proteins, leading to the activation of a pro-survival signaling pathway called unfolded protein response (UPR) (5). This adaptive response is orchestrated by three key ER stress sensors, including inositol-requiring enzyme 1 alpha (IRE1α), activating transcription factor 6 (ATF6) and PKR-like ER kinase (PERK) (6-8). IRE1α is the most conserved arm of the UPR with dual endoribonuclease and kinase activities (9). Following ER stress, the GRP78/BiP chaperone is dissociated from IRE1α, leading to IRE1α dimerization/oligomerization and subsequently the stimulation of its Kinase and RNase activities (9). The RNase activity of IRE1α splices X-box binding protein 1 (XBP1) mRNA, yielding XBP1s, a transcription factor that enhances the protein folding capacity of the ER and cellular survival (10). These ER homeostatic effects of XBP1s are mediated through the increase in the transcript levels of ER chaperones and cell fate signaling factors such as the Myc proto-oncogene (11, 12). In parallel, the RNase activity of IRE1α may mitigate protein synthesis load through the cleavage of multiple mRNAs and microRNAs in a process known as regulated IRE1-dependent decay (RIDD). However, under sever ER stress conditions, or if the UPR cannot cope with the stress, XBP1s and RIDD provoke apoptotic cell death (13, 14).

Recent reports suggest that both XBP1s and RIDD activities of the IRE1α contribute to cancer progression and drug resistance (15, 16). Therefore, finding new IRE1α modulators (both its activators and inhibitors) is considered a priority in cancer therapeutic strategies. In the drug discovery industry, short peptides emerge as promising drugs that could improve treatment options for human diseases (17, 18). For example, several peptides have been successfully used for diagnosis and treatment of cancer (19). Here, we employed a computer-aided mutation-based peptide design approach to find short peptides with the capability of targeting IRE1α activity with the hope that presenting a new generation of IRE1α modulators might be helpful for UPR-dependent diseases and drug discovery purposes.

Materials and Methods:

Modeling, structural prediction, and amino acids analysis of IRE1-IRE1 interaction

The 3D structure of the IRE1α protein was retrieved from the Protein Data Bank (PDB) (https://www.rcsb.org/) (20). Specifically, the spatial arrangement of the two monomeric units constituting the dimeric form of the IRE1α protein was identified. To find essential amino acids involved in the interaction between two IRE1 monomers, an extensive analysis of multiple articles was conducted and the PDB ID: 6W3K was selected as the basis for subsequent docking analyses. The potential glycosylation sites within the IRE1 protein were also assessed using the NetNglyc and NetOglyc tools (https://services.healthtech.dtu.dk/services/NetOGlyc-4.0/) to ensure that the strategic selection of peptides that do not interfere with these regions.

The sequences of the designed peptides were generated using the PEP-FOLD Peptide Structure Prediction Server (https://bioserv.rpbs.univ-paris-diderot.fr/services/PEP-FOLD/). These specific amino acids, along with their proximal counterparts, were chosen to form the basis of our short inhibitory peptides (21).

Docking and molecular dynamics (MD) simulation analyses

The docking analyses between the designed peptides and IRE1α protein were conducted using the HADDOCK 2.2 online server (https://alcazar.science.uu.nl/services/

HADDOCK2.2/) (22). A pivotal aspect of this analysis entailed the utilization of Ambiguous Interaction Restraints (AIR) (23). The molecular dynamics simulation of 100,000 picoseconds (ps) was conducted by employing the GROMACS 2020 package (http://gromacs.org), Gromos96 54a7 force field, and the SPCE water model. Each peptide-IRE1 complex was centered within a cubic box, ensuring a minimum distance of 1.0 nm from the box edges. To account for long-range electrostatic interactions, pressure equilibration was carried out for 1 nanosecond (ns) using the Berendsen barostat, which employs the LINCS algorithm and PME mesh calculation. Adjustments were made for Fourier grid spacing and Coulomb radius, set at 0.16 and 1.2 nm, respectively, with Van der Waals interactions configured to 1.2 nm. Upon completion of the MD simulation, 200 frames were extracted from the final 20 nanoseconds of the trajectory. Subsequently, the binding free energy of each amino acid within the peptide was computed using gmmpbsa, a GROMACS tool designed for high-throughput MM-PBSA calculations. Root Mean Square Deviation (RMSD), Radius of Gyration (Rg), Root Mean Square Fluctuations (RMSF), Surface-Accessible Surface Area (SASA), and the number of Hydrogen Bonds (H-bonds) parameters were also evaluated for each peptide (24).

Proposing new amino acids for mutation

The mCSM-PPI2 online server (https://biosig.lab.uq.edu.au/mcsm_ppi2/) was employed to suggest appropriate amino acids at the designated mutation sites (25). This server accurately predicts the impact of missense mutations on protein-protein affinity by utilizing a machine-learning approach that harnesses graph-based structural signatures termed mCSM.

Evaluation of toxicity, allergenicity, and self-assembly of designed peptides

The newly generated mutation-based peptides were subjected to rigorous scrutiny for both toxicity and allergenicity via ToxinPred (https://webs.iiitd.edu.in/raghava/toxinpred/protein.php) (26) and AllerTop (http://www.ddgpharmfac.net/AllerTOP/) (27) online servers. The self-accumulating propensity of the designed peptides was conducted using the online tool available at http://old.protein.bio.unipd.it/pasta2/work/pid_573289533/pasta.

Final peptide selection and construction of peptide library

The peptides identified through mCSM-PPI2 were subjected to further analysis and the construction of a library using OSPREY 3.0 (Open-Source Protein Redesign for You) (28). The software produces energy scores and PDB files for each peptide, enabling the selection of peptides with the highest energy scores among the generated suggestions.

Results:

IRE1α dimer structure and investigating its glycosylation points

The IRE1α protein's 3D structure was found in the PDB database (PDB ID: 6W3K). Figure 1 visually depicts the interaction involved in the IRE1α dimer. To prevent IRE1 dimerization, we should first ensured that the selected peptides did not overlap with its B2B glycosylation regions. The NetNglyc analysis revealed the presence of 2 potential N-glycosylation sites within the sequence. Specifically, these sites were identified as amino acid N in the NPTY sequence (position 204) and amino acid N in the NITV sequence (position 331). An important consideration emerged regarding the presence of a proline immediately following the N at position 204. As described in the literature, this configuration signifi-

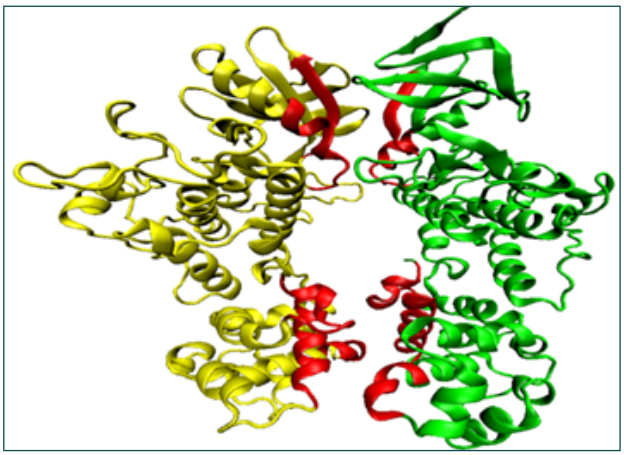

Figure 1. IRE1α dimer. The yellow and green colors demonstrate the IRE1α monomers and the red ones illustrate the hot spot amino acids involved in the interaction.

cantly diminishes the likelihood of glycosylation for this sequence. Consequently, it was determined that only position 331 retains the potential for glycosylation. Additionally, the NetOglyc results unveiled the existence of 7 possible O-glycosylation sites, denoted by amino acids at positions 2, 3, 5, 180, 183, 300, 307 and 398. Notably, none of the selected peptides were found to overlap with the identified glycosylation regions of the IRE1 protein.

Peptides designing and docking analysis

To propose peptides with the capability of targeting IRE1α, we rationally designed several short peptides based on their complementary sequence with the IRE1α-IRE1α interaction sites (Table 1). Then, all the mentioned peptides were docked against the IRE1α protein to gain their binding affinity to the protein. Among them, peptide 1 had no good affinity for the protein and was excluded from the study. The calculation of gmmpbsa showed that Cys4 and Glu6 from peptide 2, Gln8 and Ser11 from peptide3, His3, Glu6 and Leu7 from peptide4 and Glu2, Leu4, Phe5, Tyr9 and His11 from peptide5 had a negative effect on the binding affinity of peptides to IRE1α (Table 2).

Investigation of toxicity and allergenicity of peptides

At the next step, a mutation-based peptide design was performed using mCSM-PPI2. After finding suitable amino acids for each non-favorable amino acid, OSPREY was employed to make a new peptide library. Eleven peptides (three peptides for peptide-2, -3, and 4, and two peptides for peptide-5) that showed the greatest scores among others were checked for allergenicity and toxicity, then docked against IRE1α to find the best docking score for each one (Table 3).

MD simulation for the selection of best peptides

MD simulations were used to assess the stability of pro-

Table 1. Suggested peptides for inhibition of IRE1α protein.

Peptide Number	Amino acids numbers
1	614 - 624
2	627 - 634
3	836 - 851
4	906 - 914
5	953 - 963

Table 2. The energy of the peptides template residues calculated by gmmpbsa revealed by a 100-ns MD simulation.

Peptide No	Residue No	Van der Waals	Electrostatic	ΔG binding (kJ/mol)
2	Cys4	-3538.2	1518.883	5057.082
2	Glu6	3359.926	-3067.151	6427.087
3	Gln8	367.098	343.215	3767.76
3	Ser11	-466.148	1626.746	1160.604
4	His3	-580.501	918.107	338.494
4	Glu6	-224.816	53254.34	53029.528
4	Leu7	-534.265	49943.838	49409.584
5	Glu2	-4194.943	39084.965	34890.022
5	Leu4	2624.877	-2240.575	384.302
5	Phe5	769.235	5531.235	518.003
5	Tyr9	-398.724	1900.279	1501.549
5	His11	-954.29	38006.675	37061.651

Table 3. Allergenic and toxicity studies of designed peptides with the highest OSPREY scores.

Peptide Number	Peptide Sequence	OSPREY scores	Allergenicity	Toxicity
2-1	RYFRTRKD	-38.17	non-allergen	no-toxic
2-2	RYFNTRKD	-48.8	non-allergen	non
2-3	RYFRTNKD	-39.9	non-allergen	non
3-1	EKQLQFFMDVHDRIEK	-17.32	non-allergen	non
3-2	EKQLQFFHDVHDRIEK	-38.41	non-allergen	non
3-3	EKQLQFFLDVHDRIEK	-37.29	non-allergen	non
4-1	NKKHHYRMD	-26.82	non-allergen	non
4-2	NKKHHYRHD	-32.31	non-allergen	non
4-3	NKKHHYRHE	-29	non-allergen	non
5-1	HHRHFQPYYFH	-16.89	non-allergen	non
5-2	HMRHFQPYYFH	-19.09	non-allergen	non

tein-peptide complexes as well as the dynamic behaviors of peptides. Several key factors were checked to select the best peptide for each peptide number, including RMSD, RG, RMSF, SASA, and H-bonds. Peptide numbers 2-2, 3-2, 4-2, and 5-2 were the best among the designed peptides based on these above characteristics (Figures 2-6).

The RMSD changes of each atom in a molecule were calculated by comparing them with the initial structure of that molecule (Fig. 2).

RG can show the amount of compaction or folding, thus changing the properties of proteins during MD simulation and is interpreted as a characteristic of protein sta-

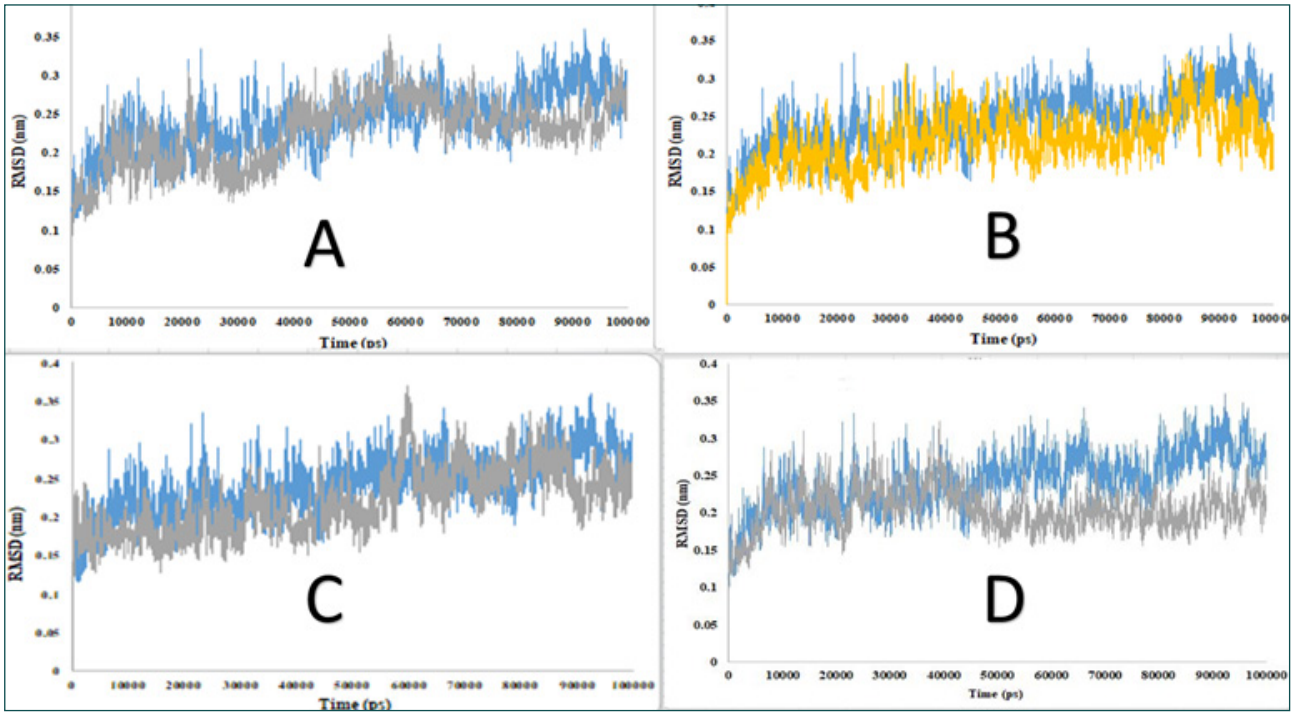

Figure 2. The RMSD graph for the entire MD simulation timescale (100000 ps (100ns)) for both the IRE1α protein and four selected peptides. A. The blue color indicates the IRE1α protein graph and the grey color shows the peptide number 2-2 graph. B. The IRE1α protein and 3-2 peptide graph are depicted in blue and yellow, respectively. In C (peptides 4–2) and D (peptides 5–2), the blue and grey colors exhibit the IRE1α protein and peptides graphs, respectively.

bility. The increase or decrease of this level indicates the abnormality of the protein and the change in its properties because each protein needs a certain amount of folding. As depicted in Fig. 3, little differences are observed in the IRE1α radius in the complex with 4 peptides and all protein-peptide complexes had constant dimensions during the simulation.

The surface-accessible surface area (SASA) is the amount of protein surface that is accessible to the solvent. The increase of this level during the simulation indicates the unfolding of parts of the protein and vice versa. The SASA plots in Fig. 4 indicate that the binding of all four peptides causes a small change in the number of superficial residues According to the findings of the RG and SASA investigations, the dimension of IRE1 remained steady following suppression by selected peptides (Fig 3 and 4).

RMSF analysis is a measure of the flexibility and fluctuation of protein amino acids and is used to distinguish unstable amino acids from stable amino acids. Fig, 5 revealed that there is little fluctuation in IRE1α residues' mobility and the fluctuation of the peptide near the end area of the graph significantly decreased (Fig. 5).

Figure 6 represents a high degree of hydrogen bonds, the main interactions that stabilize a complex, between different peptides and IRE1α protein.

Investigation of characteristics of selected peptides

Next, we conducted a comprehensive assessment of water solubility, isoelectric point, molecular weight, net charge, and self-accumulation for 4 selected peptides (Table 5). Notably, none of the peptides showed self-aggregation (Table 5), which might be due to their small sizes and lack of secondary structures, such as beta sheets (29). Among peptides, the RYFNTRKD peptide (2-2 peptide) demonstrated the least probability of self-assembly, which was estimated at -2.78.

The 3D interaction between IRE1 and wild or mutated forms of the top four peptides

Finally, the important amino acids of IRE1α protein in interaction with peptides (wild and mutated forms) have been illustrated in figures 7 and 8.

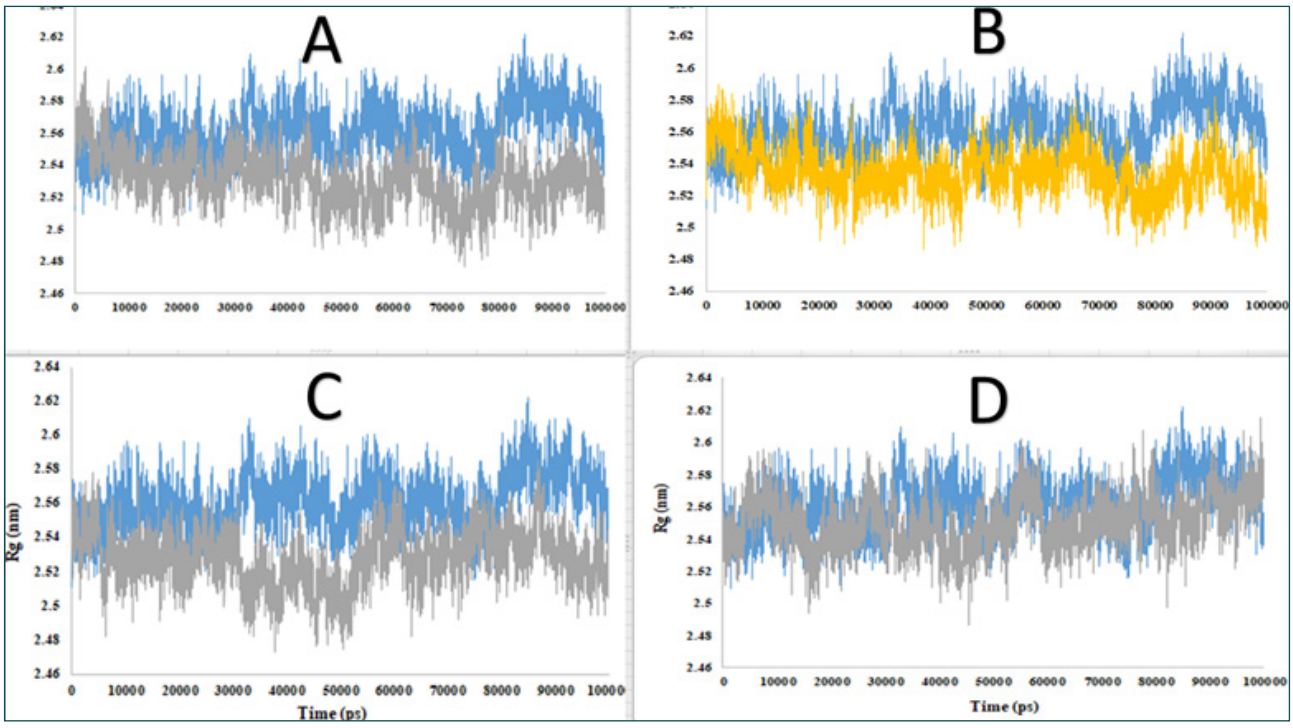

Figure 3. The RG graph for the entire MD simulation timescale (100000 ps (100 ns)) is depicted for both the IRE1α protein and four selected peptides. The blue color in all four pictures displays the IRE1α protein. The grey colors in pictures A, C, and D demonstrate the fluctuation of peptide numbers 2-2, 4-2, and 5-2, respectively. The yellow color in picture B represents the peptide number 3-2 graph.

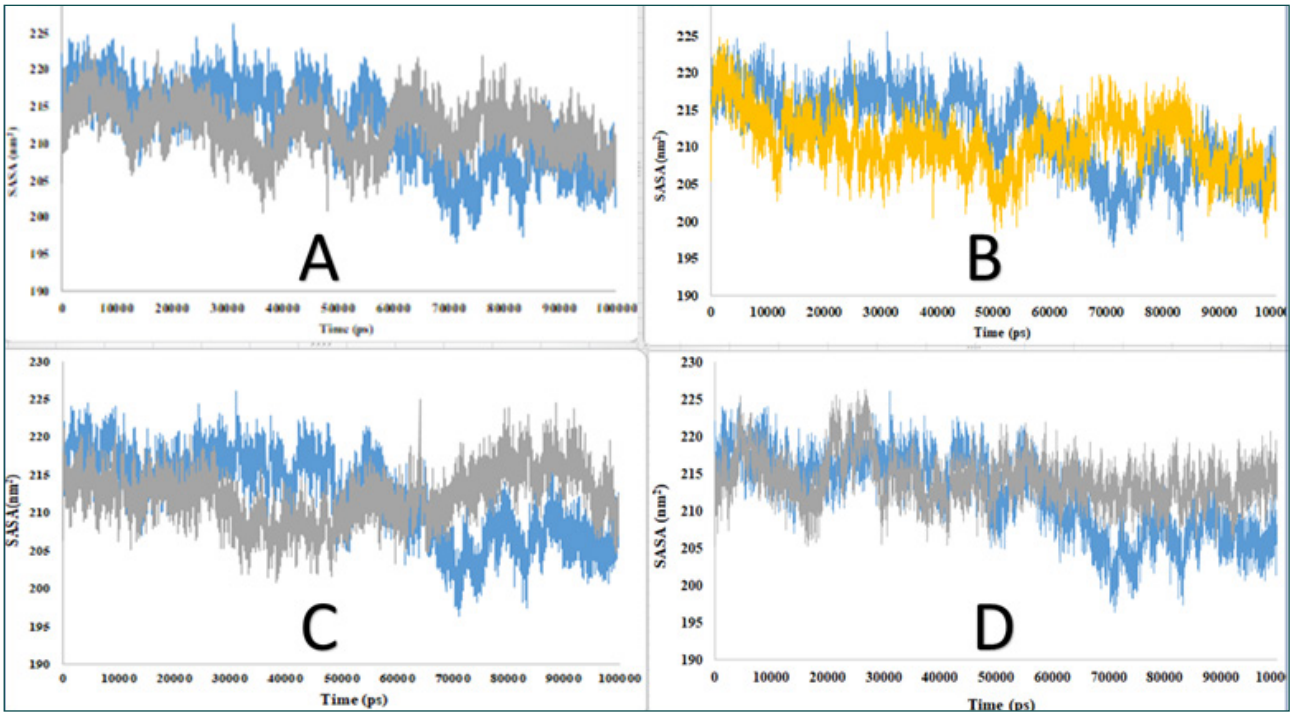

Figure 4. The SASA graph for the entire MD simulation timescale (100000 ps (100 ns)) is presented for both the IRE1α protein and four selected peptides. The blue color in all four pictures depicts the IRE1α protein. The grey colors in pictures A, C, and D show the fluctuation of peptide numbers 2-2, 4-2, and 5-2, respectively. The yellow color in picture B represents the peptide number 3-2 graph.

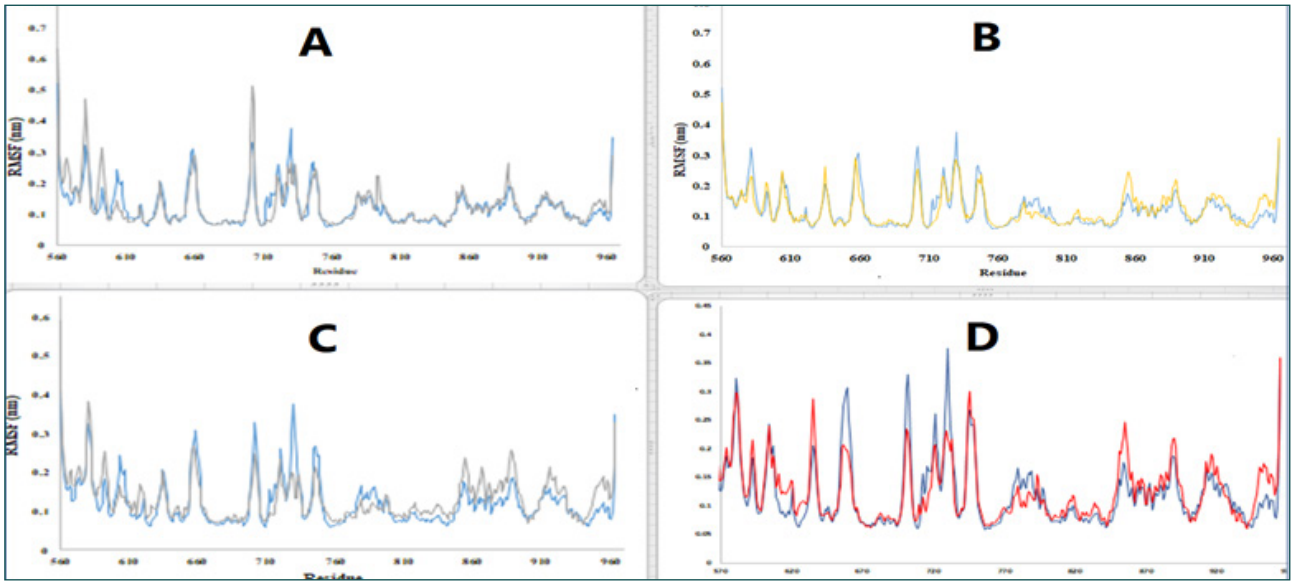

Figure 5. The RMSF graph for the entire MD simulation timescale is presented for both the IRE1α protein and four selected peptides. The blue color in all four pictures depicts the IRE1α protein. The grey colors in pictures A and C show the fluctuation of peptide numbers 2-2 and 4-2, respectively. The yellow color in picture B represents the peptide number 3-2 graph, and the peptide number 5-2 is shown as red in picture D.

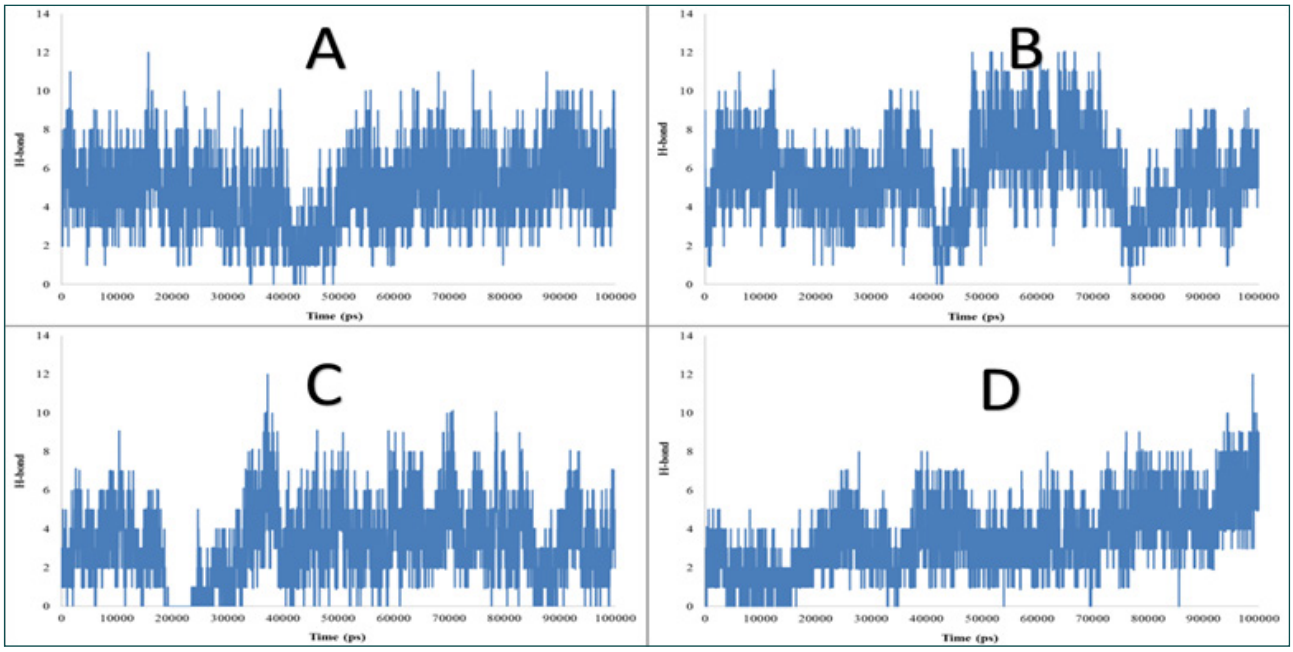

Figure 6. Estimation of the hydrogen bonds of candidate peptides. peptide number 2-2 (A), peptide number 3-2 (B), peptide number 4-2 (C), and peptide number 5-2 (D) with the IRE1α protein for 100000 ps.
As presented in Table 4, the number of H-bonds during 100 ns simulations varied for each peptide.

Table 4. The hydrogen bonds of candidate peptides with IRE1 for 100 ns.

Peptide No	Van der Waal Energy (kJ/mol)	Electrostatic Energy (kJ/mol)	Total	No. H-bond
2-2	-148.3625192	-1299.350919	-1447.713426	4.943405659
3-2	-169.3552509	-1237.020308	-1406.375548	5.609839016
4-2	-192.8133728	-1779.357434	-1932.978349	3.215178482
5-2	-194.2591144	-1139.711788	-1333.970907	1.386920582

Table 5. The molecular weight, isoelectric point, net charge, solubility, and residues involved in the interaction from IRE1α with peptides.

Peptide No	Molecular Weight (g/mol)	Isoelectric point	Net charge	Water solubility	Dock Score before mutation	Dock Score after mutation	Self- assembly
2-2	1140.6	1140.6	2.9	Good	-125.09	-150.27	No
3-2	1098.5	1098.5	1.9	Good	-111.96	-162.6	No
4-2	1233.6	1233.6	2.6	Good	-114.56	-168.16	No
5-2	1561.7	1561.7	1.6	Poor	-144.55	-170.02	No

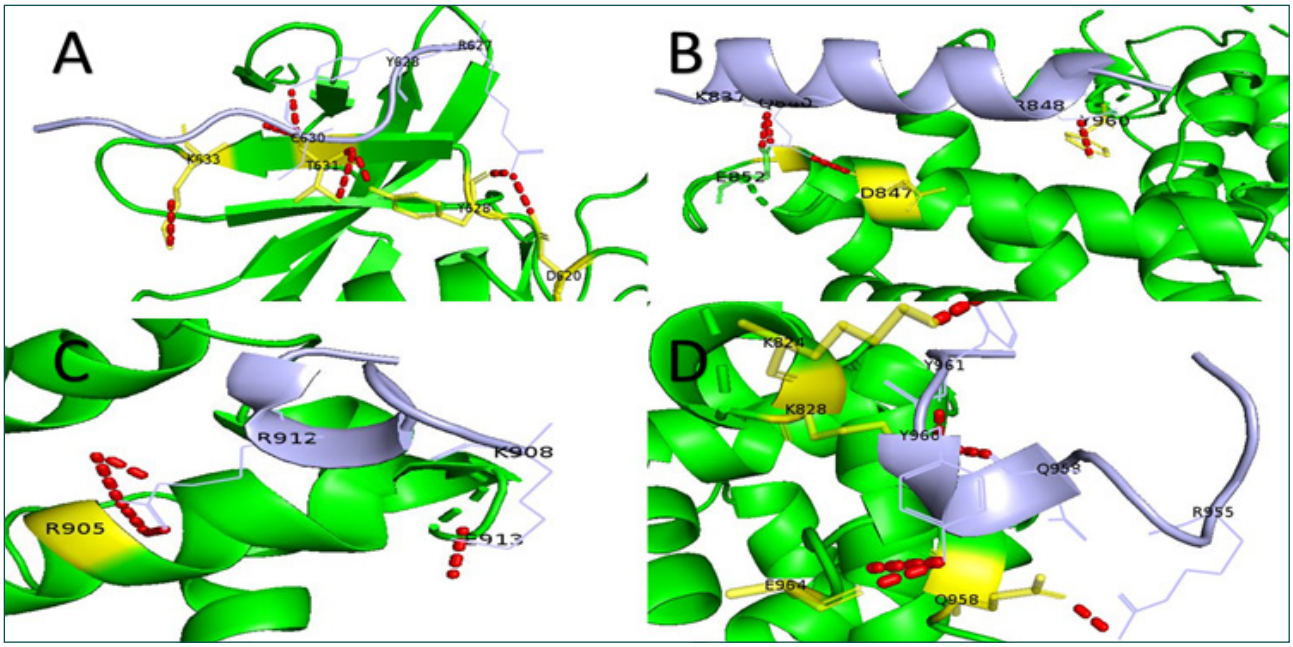

Figure 7. The 3D interaction of the optimal docking pose of the top four peptides (wild type) A) 2-2, B) 3-2, C) 4-2, and D) 5-2 bound to the IRE1 protein. The receptor is depicted in green, and peptides are shown in gray. The important amino acids involved in the interaction have been highlighted as yellow colors.

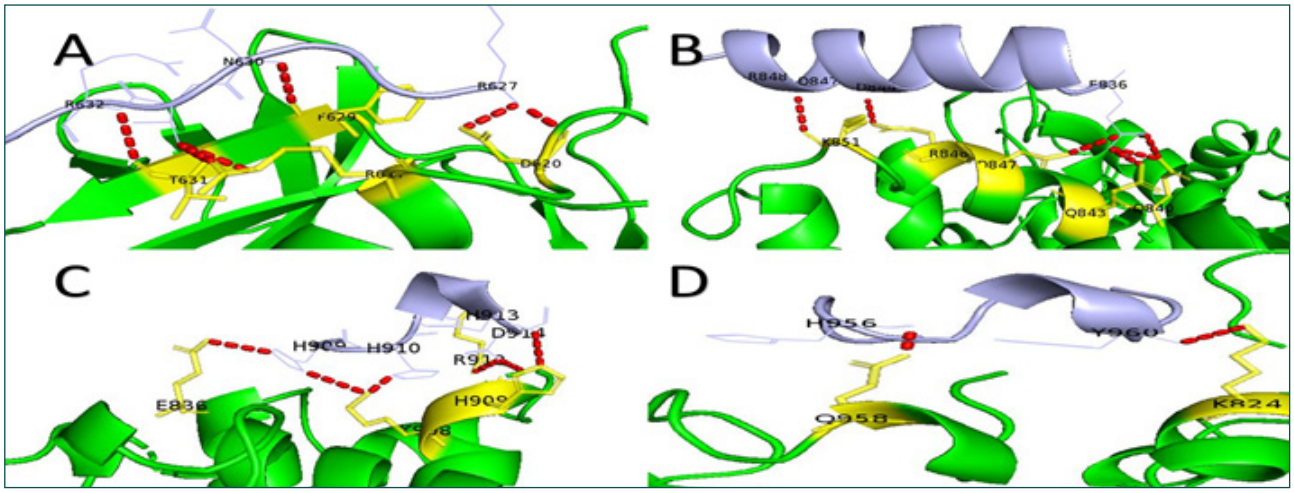

Figure 8. The 3D interaction of the optimal docking pose of the top four peptides (mutant type) A) 2-2, B) 3-2, C) 4-2, and D) 5-2 bound to the IRE1 protein. The receptor is depicted in green, and peptides are shown in gray. The important amino acids involved in the interaction have been highlighted as yellow.

Discussion:

Targeting IRE1α has shown the potential to not only reduce cancer development but also sensitize tumor cells to chemotherapies (30, 31). For instance, studies have highlighted the role of IRE1 in triple-negative breast cancer (TNBC), where the inhibition of IRE1 RNase activity in combination with chemotherapy is an effective approach to suppress tumor growth and recurrence in TNBC models (31). We also showed that RNase activity of IRE1, in particular XBP1 splicing, could be a diagnostic and/or therapeutic marker for patients with colorectal cancer (CRC) (32). Interestingly, inhibition of IRE1 by chemical tools could modulate tumor cell progression and enhance the response to chemotherapy in CRC (33).

Several compounds, such as fucoidan, 2-(3,4-dihydroxy phenyl) ethanol, and ACY-1215 have been explored for their inhibitory effects on IRE1α (34-38). Additionally, FDA-approved drugs, such as etoperidone, methotrexate, fludarabine phosphate, and folinic acid have been repurposed as potential IRE1 inhibitors (39). Inhibitors that target IRE1 activity can be categorized into kinase inhibitors (type I and II) or RNase inhibitors, based on their mechanism of action and binding sites (40). For instance, kinase inhibitor sunitinib (type I) has shown efficacy in reducing XBP1 mRNA splicing (41). Type II kinase inhibitors like (S)-2-chloro-N-(6-methyl5-((3-(2-(piperidin-3-ylamino)pyrimidin-4-yl)yridine-2-yl)oxy) naphthalen-1-yl) (42) benzenesulfonamide (18/KIRA8) (43) and N-4-[(3-2-[(trans 4-aminocyclohexyl)amino] amino] pyrimidin-4-yl}yridine-2-yl)oxy] 3 methylnaphthalen-1-yl have shown promise in the treatment of diseases and blood cancers (44). The compound 4μ8C has been identified as an effective IRE1 inhibitor, through blocking XBP1 splicing (45). Toyocamycin, derived from an Actinomycete strain, has demonstrated inhibition of IRE1-dependent XBP1 cleavage without affecting IRE1 phosphorylation (46). Combinations of inhibitors, such as MKC-8866 and nilotinib, have shown synergistic effects on cell viability in disease contexts (47). Despite these reports, finding more specific and potent modulators of IRE1 is still a matter of investigation in the drug discovery industry.

In this study, we employed a novel approach and rationally designed short peptides to specifically target IRE1α dimerization/oligomerization. Unlike previous studies that utilized long peptides or chemical compounds, short peptides offer advantages in terms of solubility, stability, delivery, and cell entrance. We report 4 mutation-based designed peptides that can interact with high scores with IRE1 oligomerization sites. Primarily, it was observed that all predicted peptides, except for peptide 5-2, exhibit favorable water solubility. This characteristic is of paramount significance when considering the selection of peptides for potential drug development. Moreover, the comprehensive assessment of allergenicity and toxicity revealed that none of the selected peptides are anticipated to evoke allergic reactions or exhibit toxic effects. Furthermore, the evaluation of critical parameters, including the number of hydrogen bonds, Van der Waals interactions, and electrostatic energy, revealed that peptides 2-2, 3-2, and 4-2 possess a robust affinity for the IRE1α protein. This robust interaction implies that these peptides are capable of forming stable complexes with the target protein, enhancing their potential as inhibitors.

Conclusion:

In summary, we identified short peptides that could inhibit IRE1α dimerization and consequently its function in silico studies. Peptides 2-2, 3-2, and 4-2, which displayed the highest affinity for IRE1α, might be considered as promising candidates for targeting IRE1 and utilizing in cancer therapeutic strategies in combination with chemotherapy. While this research predicts potential peptide candidates, translation of computational assessments to practical application requires meticulous validation of the proposed peptides' efficacy and safety. Further experimental studies are in progress in our lab to address this issue.

Abbreviation

ER: Endoplasmic Reticulum
ATF6: activating transcription factor 6
IRE1: inositol-requiring enzyme 1
PERK: PKR-like ER kinase
UPR: unfolded protein response
XBP1: X-box binding protein 1
TNBC: triple-negative breast cancer
GRP78: Glucose-regulated protein 78

Declarations

Acknowledgment:

The authors extend their sincere gratitude to the National Institute of Genetic Engineering and Biotechnology (NIGEB) for providing facilities and valuable cooperation throughout this research.

Funding:

This work has been funded by NIGEB grants to MAM, AN, and NAF. MAM is supported by the international

grant program (No: 980301-I-728) from NIGEB.

Authors contributions:

Data gathering and analyzing, writing the original draft (AG and NB), data analyzing and editing (AN), Conceptualization, data analyzing, critical editing and revising (NAF and MAM).

Ethics approval and consent to participate:

Not applicable

Consent for publication:

Not applicable

Availability of data and materials:

All data generated or analyzed during this study are included in this article and will be available as requested.

Competing Interests:

The authors have no relevant financial or non-financial interests to disclose.

REFERENCES

1. The global burden of cancer attributable to risk factors, 2010-19: a systematic analysis for the Global Burden of Disease Study 2019. Lancet. 2022;400(10352):563-91.
2. Kocarnik JM, Compton K, Dean FE, Fu W, Gaw BL, Harvey JD, et al. Cancer Incidence, Mortality, Years of Life Lost, Years Lived With Disability, and Disability-Adjusted Life Years for 29 Cancer Groups From 2010 to 2019: A Systematic Analysis for the Global Burden of Disease Study 2019. JAMA Oncol. 2022;8(3):420-44.
3. Debela DT, Muzazu SG, Heraro KD, Ndalama MT, Mesele BW, Haile DC, et al. New approaches and procedures for cancer treatment: Current perspectives. SAGE Open Med. 2021;9:20503121211034366.
4. Urra H, Dufey E, Avril T, Chevet E, Hetz C. Endoplasmic Reticulum Stress and the Hallmarks of Cancer. Trends Cancer. 2016;2(5):252-62.
5. Banerjee A, Ahmed H, Yang P, Czinn SJ, Blanchard TG. Endoplasmic reticulum stress and IRE-1 signaling cause apoptosis in colon cancer cells in response to andrographolide treatment. Oncotarget. 2016;7(27):41432.
6. Blazanin N, Son J, Craig-Lucas AB, John CL, Breech KJ, Podolsky MA, et al. ER stress and distinct outputs of the IRE1α RNase control proliferation and senescence in response to oncogenic Ras. Proceedings of the National Academy of Sciences. 2017;114(37):9900-5.
7. Yoshida H, Haze K, Yanagi H, Yura T, Mori K. Identification of the cis-acting endoplasmic reticulum stress response element responsible for transcriptional induction of mammalian glucose-regulated proteins: involvement of basic leucine zipper transcription factors. Journal of Biological Chemistry. 1998;273(50):33741-9.
8. Mori K, Ma W, Gething M-J, Sambrook J. A Transmembrane Protein with a cdc2^+/CDC28-Related Kinase Activity Is Required for Signaling from the ER to the Nucleus. CELL-CAMBRIDGE MA-. 1993;74:743-.
9. Karagöz GE, Acosta-Alvear D, Nguyen HT, Lee CP, Chu F, Walter P. An unfolded protein-induced conformational switch activates mammalian IRE1. Elife. 2017;6:e30700.
10. Wang Y, Zhang Y, Yi P, Dong W, Nalin AP, Zhang J, et al. The IL-15–AKT–XBP1s signaling pathway contributes to effector functions and survival in human NK cells. Nature immunology. 2019;20(1):10-7.
11. Sheng X, Nenseth HZ, Qu S, Kuzu OF, Frahnow T, Simon L, et al. IRE1α-XBP1s pathway promotes prostate cancer by activating c-MYC signaling. Nature communications. 2019;10(1):323.
12. Dong H, Adams NM, Xu Y, Cao J, Allan DS, Carlyle JR, et al. The IRE1 endoplasmic reticulum stress sensor activates natural killer cell immunity in part by regulating c-Myc. Nature immunology. 2019;20(7):865-78.
13. Chen S, Chen J, Hua X, Sun Y, Cui R, Sha J, et al. The emerging role of XBP1 in cancer. Biomedicine & Pharmacotherapy. 2020;127:110069.
14. Chen Y, Brandizzi F. IRE1: ER stress sensor and cell fate executor. Trends in cell biology. 2013;23(11):547-55.
15. Hollien J, Weissman JS. Decay of endoplasmic reticulum-localized mRNAs during the unfolded protein response. Science. 2006;313(5783):104-7.

16. Han D, Lerner AG, Vande Walle L, Upton JP, Xu W, Hagen A, et al. IRE1alpha kinase activation modes control alternate endoribonuclease outputs to determine divergent cell fates. Cell. 2009;138(3):562-75.
17. Karami Fath M, Babakhaniyan K, Zokaei M, Yaghoubian A, Akbari S, Khorsandi M, et al. Anti-cancer peptide-based therapeutic strategies in solid tumors. Cellular & Molecular Biology Letters. 2022;27(1):33.
18. J Boohaker R, W Lee M, Vishnubhotla P, LM Perez J, R Khaled A. The use of therapeutic peptides to target and to kill cancer cells. Current medicinal chemistry. 2012;19(22):3794-804.
19. Shapira S, Fokra A, Arber N, Kraus S. Peptides for diagnosis and treatment of colorectal cancer. Current medicinal chemistry. 2014;21(21):2410-6.
20. Kouranov A, Xie L, de la Cruz J, Chen L, Westbrook J, Bourne PE, et al. The RCSB PDB information portal for structural genomics. Nucleic acids research. 2006;34(suppl_1):D302-D5.
21. Adams CJ, Kopp MC, Larburu N, Nowak PR, Ali MM. Structure and molecular mechanism of ER stress signaling by the unfolded protein response signal activator IRE1. Frontiers in molecular biosciences. 2019;6:11.
22. Van Zundert G, Rodrigues J, Trellet M, Schmitz C, Kastritis P, Karaca E, et al. The HADDOCK2. 2 web server: user-friendly integrative modeling of biomolecular complexes. Journal of molecular biology. 2016;428(4):720-5.
23. Dominguez C, Boelens R, Bonvin AM. HADDOCK: a protein− protein docking approach based on biochemical or biophysical information. Journal of the American Chemical Society. 2003;125(7):1731-7.
24. Kumari R, Kumar R, Consortium OSDD, Lynn A. g_mmpbsa□ A GROMACS tool for high-throughput MM-PBSA calculations. Journal of chemical information and modeling. 2014;54(7):1951-62.
25. Rodrigues CH, Myung Y, Pires DE, Ascher DB. mCSM-PPI2: predicting the effects of mutations on protein–protein interactions. Nucleic acids research. 2019;47(W1):W338-W44.
26. Gupta S, Kapoor P, Chaudhary K, Gautam A, Kumar R, Consortium OSDD, et al. In silico approach for predicting toxicity of peptides and proteins. PloS one. 2013;8(9):e73957.
27. Dimitrov I, Bangov I, Flower DR, Doytchinova I. AllerTOP v. 2—a server for in silico prediction of allergens. Journal of molecular modeling. 2014;20:1-6.
28. Hallen MA, Martin JW, Ojewole A, Jou JD, Lowegard AU, Frenkel MS, et al. OSPREY 3.0: open-source protein redesign for you, with powerful new features. Journal of computational chemistry. 2018;39(30):2494-507.
29. Gee J, Shell MS. Two-dimensional replica exchange approach for peptide–peptide interactions. The Journal of chemical physics. 2011;134(6).
30. Sheng X, Arnoldussen YJ, Storm M, Tesikova M, Nenseth HZ, Zhao S, et al. Divergent androgen regulation of unfolded protein response pathways drives prostate cancer. EMBO molecular medicine. 2015;7(6):788-801.
31. Logue SE, McGrath EP, Cleary P, Greene S, Mnich K, Almanza A, et al. Inhibition of IRE1 RNase activity modulates the tumor cell secretome and enhances response to chemotherapy. Nature communications. 2018;9(1):3267.
32. Zarafshani M, Mahmoodzadeh H, Soleimani V, Moosavi MA, Rahmati M. Expression and Clinical Significance of IRE1-XBP1s, p62, and Caspase-3 in Colorectal Cancer Patients. Iranian Journal of Medical Sciences. 2023.
33. Abbasi S, Rivand H, Eshaghi F, Moosavi MA, Amanpour S, McDermott MF, et al. Inhibition of IRE1 RNase activity modulates tumor cell progression and enhances the response to chemotherapy in colorectal cancer. Medical Oncology. 2023;40(9):247.
34. Maurel M, McGrath EP, Mnich K, Healy S, Chevet E, Samali A, editors. Controlling the unfolded protein response-mediated life and death decisions in cancer. Seminars in cancer biology; 2015: Elsevier.
35. Yoneda T, Imaizumi K, Oono K, Yui D, Gomi F, Katayama T, et al. Activation of caspase-12, an endoplastic reticulum (ER) resident caspase,

through tumor necrosis factor receptor-associated factor 2-dependent mechanism in response to the ER stress. Journal of Biological Chemistry. 2001;276(17):13935-40.
36. Drogat B, Auguste P, Nguyen DT, Bouchecareilh M, Pineau R, Nalbantoglu J, et al. IRE1 signaling is essential for ischemia-induced vascular endothelial growth factor-A expression and contributes to angiogenesis and tumor growth in vivo. Cancer research. 2007;67(14):6700-7.
37. Chen S, Zhao Y, Zhang Y, Zhang D. Fucoidan induces cancer cell apoptosis by modulating the endoplasmic reticulum stress cascades. PloS one. 2014;9(9):e108157.
38. Guichard C, Pedruzzi E, Fay M, Marie J-C, Braut-Boucher F, Daniel F, et al. Dihydroxyphenylethanol induces apoptosis by activating serine/threonine protein phosphatase PP2A and promotes the endoplasmic reticulum stress response in human colon carcinoma cells. Carcinogenesis. 2006;27(9):1812-27.
39. Doultsinos D, Carlesso A, Chintha C, Paton JC, Paton AW, Samali A, et al. Peptidomimetic-based identification of FDA-approved compounds inhibiting IRE1 activity. The FEBS journal. 2021;288(3):945-60.
40. Siwecka N, Rozpędek-Kamińska W, Wawrzynkiewicz A, Pytel D, Diehl JA, Majsterek I. The structure, activation and signaling of IRE1 and its role in determining cell fate. Biomedicines. 2021;9(2):156.
41. Ali MM, Bagratuni T, Davenport EL, Nowak PR, Silva-Santisteban MC, Hardcastle A, et al. Structure of the Ire1 autophosphorylation complex and implications for the unfolded protein response. The EMBO journal. 2011;30(5):894-905.
42. Zhang D, De Veirman K, Fan R, Jian Q, Zhang Y, Lei L, et al. ER stress arm XBP1s plays a pivotal role in proteasome inhibition-induced bone formation. Stem cell research & therapy. 2020;11(1):1-13.
43. Harnoss JM, Le Thomas A, Shemorry A, Marsters SA, Lawrence DA, Lu M, et al. Disruption of IRE1α through its kinase domain attenuates multiple myeloma. Proceedings of the National Academy of Sciences. 2019;116(33):16420-9.
44. 44. Cross BC, Bond PJ, Sadowski PG, Jha BK, Zak J, Goodman JM, et al. The molecular basis for selective inhibition of unconventional mRNA splicing by an IRE1-binding small molecule. Proceedings of the National Academy of Sciences. 2012;109(15):E869-E78.
45. 45. Sun H, Lin D-C, Guo X, Masouleh BK, Gery S, Cao Q, et al. Inhibition of IRE1α-driven pro-survival pathways is a promising therapeutic application in acute myeloid leukemia. Oncotarget. 2016;7(14):18736.
46. 46. Vieri M, Preisinger C, Schemionek M, Salimi A, Patterson JB, Samali A, et al. Targeting of BCR-ABL1 and IRE1α induces synthetic lethality in Philadelphia-positive acute lymphoblastic leukemia. Carcinogenesis. 2021;42(2):272-84.
47. 47. Papandreou I, Denko NC, Olson M, Van Melckebeke H, Lust S, Tam A, et al. Identification of an Ire1alpha endonuclease specific inhibitor with cytotoxic activity against human multiple myeloma. Blood, The Journal of the American Society of Hematology. 2011;117(4):1311-4.